

An Experimental Study of Turbulent Boundary Layer over 2D Transverse Circular Bars

Md Kamruzzaman, K. M. Talluru, L. Djenidi and R. A. Antonia

School of Engineering
 The University of Newcastle, NSW 2308, Australia

Abstract

In this paper, we present the results from a turbulent boundary layer developing over a rough surface. The surface consists of transverse cylindrical rods (k , the rod diameter) that are periodically arranged in the streamwise direction with a spacing of $\lambda/k = 8$ (λ is the distance between two adjacent roughness elements), that results in maximum form drag. Particular attention is paid to the measurement of the friction velocity (U_τ) that plays a major role in the assessment of the roughness effects on the flow. Hot-wire anemometry is used to measure the mean and fluctuating velocity components and pressure tap measurements are carried out to obtain the drag. Two methods are used to determine U_τ . One is based on the momentum integral equation. The second relies on measuring the pressure distribution around one roughness element. Results show that both methods give consistent values for U_τ to within 3%. Further, the drag coefficient (C_D) is observed to be independent of the Reynolds number.

Introduction

In turbulence research, significant experimental work has been carried out in understanding the turbulent boundary layers developing over smooth surfaces with zero-pressure gradient. In comparison, the rough wall studies have received far less attention due to the difficulties associated with conducting experiments over rough surfaces. This disparative approach has inhibited the contribution of rough wall studies in attempts to answer some of the fundamental issues in boundary layer research. Besides, there are engineering incentives in understanding flows over rough surfaces to benefit from increased heat and mass transfer rates and greater momentum transport across the boundary layer.

The two prominent difficulties in rough wall experiments are: (i) the uncertainty in estimating the friction velocity ($U_\tau = \sqrt{\tau_w/\rho}$, where, τ_w is the wall shear stress and ρ is the density of the fluid); see [2; 7] and (ii) determining accurately the origin in the wall-normal direction [4]. Furthermore, there are added difficulties in measuring the mean Reynolds shear stress $-\overline{uv}$ (the overline denotes time averaging) atleast in hot-wire anemometry; see, for example, [2; 7; 13]. Often, U_τ^2 is assumed to be equal to the maximum of $-\overline{uv}$. Unfortunately, when the rough wall is made up of 2D transverse elements, the distribution of $-\overline{uv}$ measured with X-wires decreases abnormally as the wall is approached (e.g. [2; 10; 5; 7; 13]). Such behaviour is not observed in hot wire measurements over a rough wall consisting of a woven mesh [7]. [1] argued that such difficulties may be responsible for discrepancies in the results which may have contributed to the outer layer ‘‘controversy’’, *i.e.*, whether or not the outer region of the boundary layer is affected by the rough wall. For example, the available data, mostly at sufficiently large Reynolds numbers and δ/k ($\delta \equiv \delta_{99}$ and k are the boundary layer thickness and characteristic roughness height, respectively) seem to suggest that 3D and transverse 2D rough surfaces may affect the outer layer differently [14]. This issue can only be resolved once U_τ and $-\overline{uv}$ can be measured accurately and independently on the 2D rough walls.

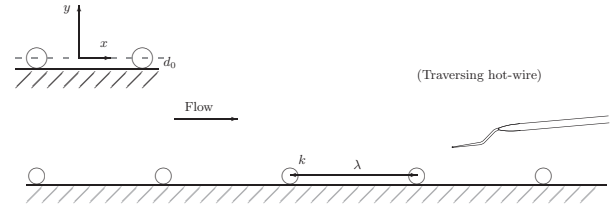


Figure 1: A schematic of the experimental set-up. The inset shows the coordinate system and the virtual origin.

With this motivation, we present our attempts here, to measure U_τ using the pressure distribution around the roughness element. The basis of this technique is one of the results reported in [9]. In their simulation study of a turbulent channel flow with square bars on one of the walls, they highlighted that $\lambda/k = 8$ is the critical value beyond which the flow pattern in the neighbourhood of the roughness elements remained essentially unchanged. Further, the viscous drag is negligible when averaged over one wavelength of the roughness elements. Hence, a spacing of $\lambda/k = 8$ is adopted in this study. This simplifies the estimation of U_τ since for $\lambda/k = 8$, the total drag is contributed solely by the pressure drag. A description of the method is presented in section 4 of the paper.

Details of the Experiments

Experiments are carried out in a boundary layer wind tunnel, whose full details are given in [6]. The boundary layer develops over a rough surface consisting of transverse cylindrical rods ($k = 1.6$ mm), a schematic is shown in figure 1. The experimental set-up is similar to that used in [13], however, with one significant difference. The roughness elements are arranged in the streamwise direction with a spacing of $\lambda/k = 8$ in this study as compared to $\lambda/k = 4$ used by [13]. The free stream velocity is set close to 14 m/s, and the measurements are conducted at five different streamwise stations between 1.4 m and 2.8 m downstream of the trip. The mean pressure gradient is maintained to be less than 0.1% across the entire working section of the wind tunnel. At each of these stations, hot-wire measurements are taken at 40 logarithmically spaced stations between $1 < z < 100$ mm. The boundary layer properties at these measurement locations are summarised in table 1. Relatively large

x (m)	δ_{99} (m)	δ^* (m)	θ (m)	Re_τ	Re_θ
1.48	0.059	0.0168	0.0091	3460	8120
1.94	0.076	0.0214	0.0119	4410	10500
2.24	0.077	0.0222	0.0126	4480	11100
2.54	0.091	0.0244	0.0140	5300	12600
2.84	0.10	0.0268	0.0154	5830	14100

Table 1: Boundary layer properties at different streamwise locations at a constant free stream velocity of 14 m/s.

values of δ/k in the range 36-62 are achieved in this study.

The probes used for these experiments are built in-house with a prong spacing of 1.5 mm. The sensor is formed from the etched portion of a Wollaston wire to reveal a 2.5 μm diameter Platinum-Rhodium (10% Rh) alloy core of length 0.5 mm (corresponding to an $l^+ \approx 26$). The hot-wire is operated with an OHR of 1.5 using an in-house developed constant temperature anemometer. In this paper, x and y refer to the streamwise and wall-normal directions while, u and v respectively denote the corresponding fluctuating velocity components.

Pressure Distribution Around a Two-Dimensional Rod

As explained in the introduction, we obtained U_τ by measuring the pressure distribution around the roughness element. For this, one of the roughness elements is replaced by a hollow cylindrical rod of identical diameter with a small circular hole drilled on its surface. The hole has a diameter of 0.3 mm and acts as a static pressure tap. The inset of figure 2 shows the schematic of this arrangement where the angle α is measured in the clockwise direction with zero angle defined when the static port is directly facing the flow. One end of the hollow cylindrical rod is closed, and the static pressure is measured via the other end. By rotating the tube through 2π radians, we obtain the pressure distribution around the circumference of the roughness element.

Tests have been carried out using this arrangement at different speeds ranging between 8 m/s and 16 m/s, and the results of the normalised static pressure are shown in figure 2. Interestingly, there is a complete collapse of all the profiles suggesting that the drag coefficient (C_D) has become independent of the Reynolds number, as can be seen from table 2. Here, C_D is obtained [3] from the pressure drag (F_D) acting per unit length of the rod, i.e.

$$C_D = \frac{2F_D}{\rho U_\infty^2 k}, \quad (1)$$

where F_D is,

$$F_D = \int_0^{2\pi} \frac{1}{2} p_s k \cos\alpha \, d\alpha. \quad (2)$$

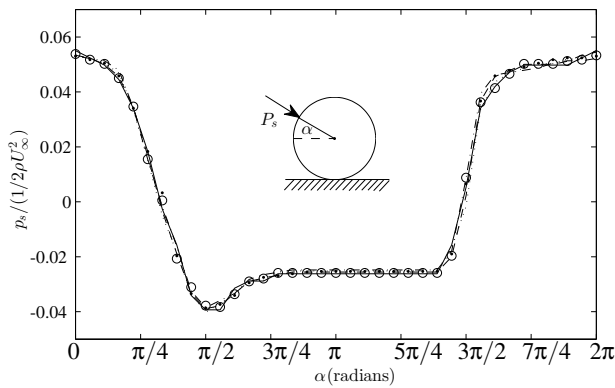


Figure 2: Distribution of the normalised static pressure around the rod at different free stream velocities ranging between 8 ms^{-1} and 16 ms^{-1} . The inset shows the arrangement for measuring the pressure distribution using the static pressure port on a rotatable hollow rod.

Estimating U_τ

For the estimation of U_τ , two methods have been considered in this study. In the first method, we exploit the specific configuration of roughness elements used in our experiments. In general the total friction coefficient C_f is equal to the sum of C_p (form drag) and C_v (viscous drag). Here C_v and C_p are respectively given by,

$$C_v = \frac{2}{\rho U_\infty^2 \lambda} \int_0^{2\pi} \frac{\partial U}{\partial y} \, ds \quad (3)$$

and

$$C_p = \frac{2}{\rho U_\infty^2 \lambda} \int_0^{2\pi} p_s \hat{\mathbf{n}} \cdot \mathbf{x} \, ds, \quad (4)$$

where, $\hat{\mathbf{n}}$ is the unit normal to the surface, \mathbf{x} is the unit vector in the stream-wise direction and s is the curvilinear coordinate. Equation 4 can be written as,

$$C_p = \frac{k}{\rho U_\infty^2 \lambda} \int_0^{2\pi} p_s \cos\alpha \, d\alpha \equiv \frac{C_D}{\lambda/k}. \quad (5)$$

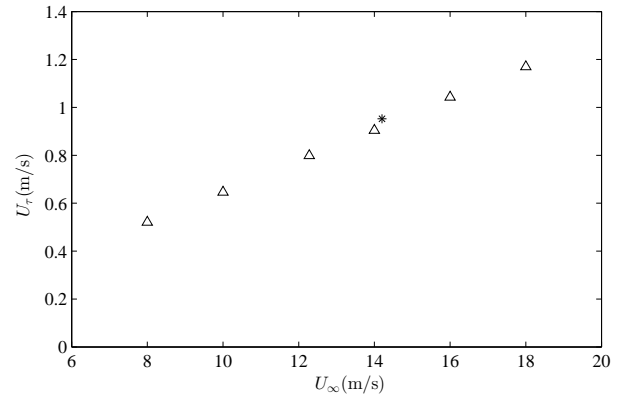


Figure 3: Values of U_τ (symbol Δ) inferred from the static pressure distribution around one element at different free stream velocities between 8 m/s and 16 m/s. Also shown as (*) is the U_τ estimate from the momentum integral equation.

However, as highlighted by [9], $\lambda/k = 8$ has a negligible contribution of C_v to C_f , when averaged across one roughness wavelength. Hence, C_p is equivalent to C_f , thereby enabling us to calculate U_τ based on C_D as,

$$U_\tau = U_\infty \sqrt{\frac{C_D}{2(\lambda/k)}} = U_\infty \sqrt{\frac{C_f}{2}}. \quad (6)$$

Velocity (ms^{-1})	C_D	$U_\infty \sqrt{(\frac{d\theta}{dx})}$	U_τ (ms^{-1})	Re_τ	Re_θ
8.05	0.067	-	0.52	3000	6950
10.10	0.067	-	0.65	3610	8480
12.15	0.067	-	0.80	4760	11000
14.00	0.067	0.91	0.94	5300	12630
15.95	0.068	-	1.04	6310	14580

Table 2: Results obtained using pressure measurements at different free stream velocities ranging between 8 m/s and 16 m/s.

Using the above procedure, U_τ has been obtained at various free stream velocities between 8 m/s and 16 m/s. The results are shown in figure 3 and are tabulated in table 2. It is easy to infer that U_τ increased linearly with U_∞ . To validate these results, we obtained U_τ through a second method, namely, the Von-Karman momentum integral equation in a zero-pressure gradient boundary layer as,

$$\frac{U_\tau^2}{U_\infty^2} = \frac{C_f}{2} = \frac{d\theta}{dx}, \quad (7)$$

where θ is the momentum thickness. Note that the contribution from the normal stresses is neglected here. From the measurements at five different streamwise locations, we have been able to obtain the variation of θ as a function of x and is shown in figure 4. It is noted that θ varied approximately in a linear fashion with x . The slope of its variation gives $\frac{d\theta}{dx}$ from which U_τ has been determined using equation 7. This value of U_τ is presented in figure 3 to compare against the results from pressure measurements. We observe that both methods gave U_τ values to within 3%. This small error highlights the merit of the pressure measurement technique used in this study.

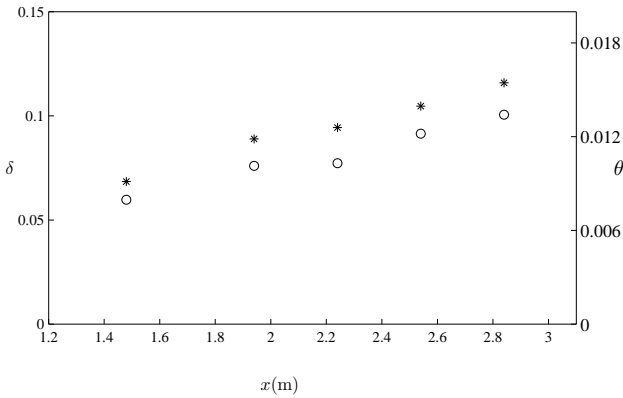


Figure 4: Variation of boundary layer thickness (δ , symbol *) and momentum thickness (θ , symbol O) as a function of streamwise distance (x).

Estimating the Virtual Origin for the Rough wall

A second prominent issue in rough wall boundary layers surrounds the accurate determination of the location of the effective origin for the wall. In determining the displacement height, d_0 (measured from the wall), most studies assume implicitly that the slope of the logarithmic region in the mean velocity profile is same in both smooth and rough walls. To avoid such assumptions, we adopt here the scheme given by [4]. In this approach, we determine d_0 by calculating the centroid of the pressure moments acting on the roughness element. The net moment (M) acting per unit length of the roughness element is calculated from the static pressure distribution as,

$$M = \int_0^{2\pi} p_s \cos\alpha \left(\frac{k}{2} + \frac{k}{2} \sin\alpha \right) \frac{k}{2} d\alpha, \quad (8)$$

and the displacement height is obtained as, $d_0 = M/F_D$. Note that the moments are taken with respect to the wall. It is observed that d_0/k remained unchanged for a range of free stream velocities, $8 \text{ m/s} \leq U_\infty \leq 16 \text{ m/s}$. This is somewhat expected following our previous observation, where it was noticed that the normalised static pressure around the roughness element remained the same for a range of U_∞ values. We obtained a value

of $d_0/k = 0.45$, slightly lower than the value ($d_0/k = 0.48$) reported by [9] for the same configuration ($\lambda/k = 8$) of roughness elements. The difference is due to the different shapes of roughness elements; square bars are used in [9] as different to circular rods used here.

Thus far, we have discussed how d_0 and U_τ are obtained without making any prior assumptions about the mean velocity profile in a boundary layer. With this background, we can now study how the statistics over smooth and rough wall boundary layers compare, in particular, the mean velocity profile.

Mean Velocity and Velocity Defect

The mean velocity profiles at five streamwise locations are shown in figure 5(a). Here U and y are normalised using inner-scales as, $U^+ = U/U_\tau$ and $y^+ = yU_\tau/\nu$. It is to be noted that the wall-normal variable y is the adjusted wall position as, $y = y - d_0$. The smooth wall data (at a comparable Re) from a different boundary layer ($U_\infty = 20.1 \text{ m/s}$, $U_\tau = 0.71 \text{ m/s}$, $\delta = 0.073 \text{ m}$ and $Re_\theta = 10900$ [8]) is used for the purpose of comparison. Note that the previously observed trend of C_f being independent of Re_θ (see table 2) supports the fully rough conditions in this study [12]. Looking at figure 5(a), it appears that the mean velocity profiles in smooth and rough walls exhibit a logarithmic behavior. However, they exhibit different slopes. The two dashed lines shown in figure 5(a) have the same slope, and it is clear that it does not represent the slope of the log-region over rough walls. Furthermore, there is a good collapse of all the inner-normalised mean velocity profiles beyond $x = 1.94 \text{ m}$. This seems to suggest the use of U_τ as a scaling parameter is more justified for rough walls than for smooth wall flows.

Figure 5(b) presents the mean velocity profiles over the smooth and rough walls in the velocity defect form ($(U_\infty - U)/U_\tau$ versus y/δ_{99}). It is clear that there are considerable differences in the region close to the wall, whilst there is good collapse beyond $y/\delta \geq 0.2$ (see the inset in figure 5(b)). The differences observed in the outer region in figure 5(a) are not visible in figure 5(b), where y is normalised by δ instead of ν/U_τ . This suggests that δ is a better scaling parameter for length, at least, in rough walls. More importantly, the velocity defect profiles over rough walls have a different slope compared to the smooth wall data. This is in contrary to the results reported in [7] and we believe that the differences are due to the ambiguity in determining U_τ . [7] used the profile matching method described in [6] to obtain U_τ , where they assumed a constant slope value for the log-regions in smooth and rough walls, an assumption which may be questionable.

To elucidate further the difference in the slopes of the log-region in smooth and rough walls, we plot the indicator parameter, $y^+ \frac{dU^+}{dy^+}$ as a function of y^+ in figure 5(c) (only the data at $x = 2.24 \text{ m}$ is shown here for brevity). The indicator, when applied to experimental data, shows a plateau region (its magnitude is equivalent to $1/\kappa$, κ is the Karman constant), representing the logarithmic behaviour of the velocity profile. We observe that both smooth and rough wall data only exhibit a seemingly plateau region. However, the levels are vividly different. The rough wall data shows a lower plateau, implying a higher value of κ . This seems to suggest that the Karman constant may depend on the surface roughness and hence challenges the concept of the roughness function (ΔU^+), generally used in assessing the effect of the roughness on the boundary layer (because ΔU^+ is obtained by assuming a constant slope for the log-region in smooth and rough wall flows [11]). These observations remain of a preliminary nature and need to be confirmed by further measurements over a bigger range of x .

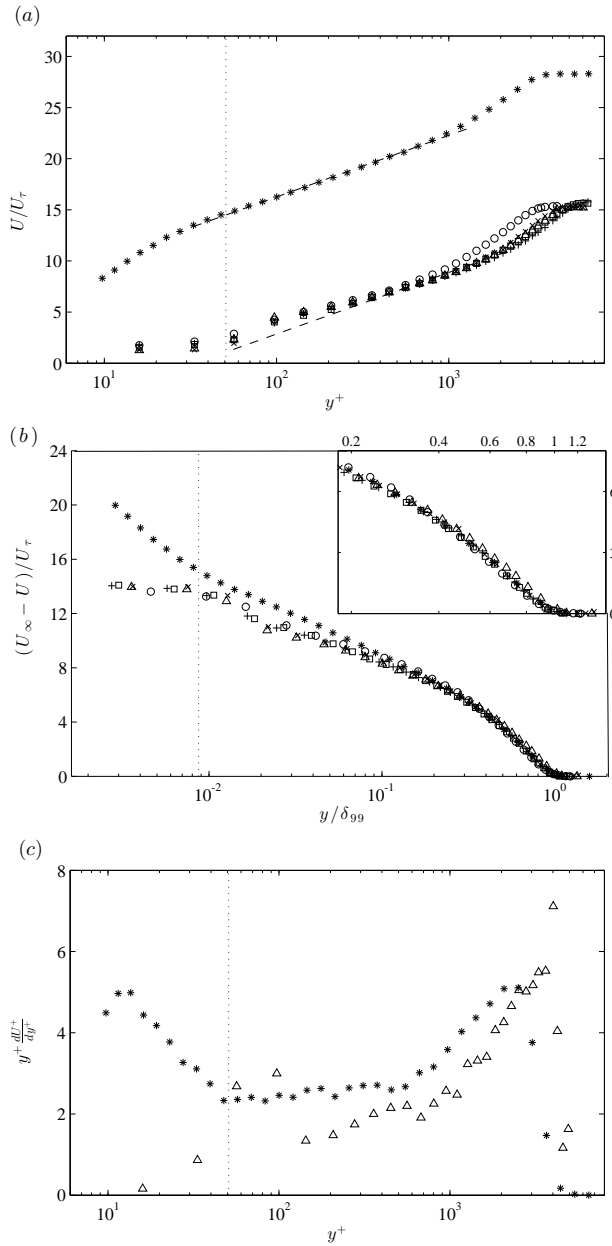


Figure 5: Comparison of mean velocity profiles between the (*) smooth wall data [8] and the present rough wall data. (a) Inner scaling; (b) Velocity defect scaling; (c) Test function $y^+ \frac{dU^+}{dy^+}$. Symbols are; (O) $x = 1.48$ m, (x) $x = 1.94$ m, (Δ) $x = 2.24$ m, (\square) $x = 2.54$ m and (+) $x = 2.84$ m. The vertical dotted line indicates the physical extent of the roughness element.

Conclusions

Two types of measurement techniques namely, static pressure and hot wire anemometry were carried out to estimate U_τ over rough walls. Both methods produce closely agreeing results. The static pressure distribution around the circular roughness elements is unchanged over a range of Re . As a consequence, the displacement height (d_0) is also unchanged over this range. The mean velocity and the velocity defect profiles showed a good collapse when scaled with U_τ and δ , indicating that they are better scaling parameters for rough walls. Comparison of the mean velocity profiles over smooth and rough walls implies that they have different κ values, with the caveat that a “true” value of κ may not exist. The present results challenge the valid-

ity of the roughness function generally used to assess the roughness effects. As a concluding note, the exact determination of U_τ and d_0 as presented in this study, will aid in clarifying the ongoing discussion about the validity of outer-layer similarity hypothesis in smooth and rough wall boundary layer flows.

Acknowledgements

We gratefully acknowledge the Australian Research Council for the financial support of this work. We thank Mr. Tom Bryon for his technical assistance in the lab.

References

- [1] Antonia, R. A. and Djenidi, L., On the outer layer controversy for a turbulent boundary layer over a rough wall, in *IUTAM symposium on the physics of wall-bounded turbulent flows on rough walls*, Springer, 2010, 77-86.
- [2] Antonia, R. A. and Luxton, R. E., The response of a turbulent boundary layer to a step change in surface roughness part 1. smooth to rough, *J. Fluid Mech.*, **48**, 1971, 721–761.
- [3] Furuya, Y., Miyata, M. and Fujita, H., Turbulent boundary layer and flow resistance on plates roughened by wires, *J. Fluids Eng.*, **98**, 1976, 635–643.
- [4] Jackson, P. S., On the displacement height in the logarithmic velocity profile, *J. Fluid Mech.*, **111**, 1981, 15–25.
- [5] Kameda, T., Osaka, H. and Mochizuki, S., Mean flow quantities for the turbulent boundary layer over a k-type rough wall, *13th Adust. Fluid Mech. Conf., Monash University, Melbourne*, 357–360.
- [6] Krogstad, P. A., Antonia, R. A. and Browne, L. W. B., Comparison between rough-and smooth-wall turbulent boundary layers, *J. Fluid Mech.*, **245**, 1992, 599–617.
- [7] Krogstad, P. A. and Antonia, R. A., Surface roughness effects in turbulent boundary layers, *Exp. Fluids*, **27**, 1999, 450–460.
- [8] Kulandaivelu, V., *Evolution of zero pressure gradient turbulent boundary layers from different initial conditions*, PhD Thesis, The University of Melbourne, 2012.
- [9] Leonardi, S., Orlandi, P., Smalley, R. J., Djenidi, L. and Antonia, R. A., Direct numerical simulations of turbulent channel flow with transverse square bars on one wall, *J. Fluid Mech.*, **491**, 2003, 229–238.
- [10] Mulhearn, P. J. and Finnigan, J. J., Turbulent flow over a very rough, random surface, *Boundary-Layer Meteorol.*, **15**, 1978, 109–132.
- [11] Perry, A. E., Schofield, W. H. and Joubert, P. N., Rough wall turbulent boundary layers, *J. Fluid Mech.*, **37**, 1969, 383–413.
- [12] Schlichting, H. and Gersten, K., *Boundary-layer theory*, Springer, 2000.
- [13] Smalley, R. J., Antonia, R. A. and Djenidi, L., Self-preservation of rough-wall turbulent boundary layers, *Euro. J. Mech.-B/Fluids*, **20**, 2001, 591–602.
- [14] Volino, R. J., Schultz, M. P. and Flack, K. A., Turbulence structure in boundary layers over periodic two-and three-dimensional roughness, *J. Fluid Mech.*, **676**, 2011, 172–190.